Asia-Pacific Journal of Science and Technology: Volume: 27. Issue: 05. Article ID.: APST-27-05-10. Research Article

APST

Asia-Pacific Journal of Science and Technology

https://www.tci-thaijo.org/index.php/APST/index

Published by the Research and Technology Transfer Affairs Division,
Khon Kaen University, Thailand

# Investigation of mangosteen $^{1}$H-NMR relaxation properties aims for detection of translucent flesh disorder

Suriya Chinwong[1] and Nath Saowadee[1,*]

[1]Department of Physics, Faculty of Science, Khon Kaen University, Khon Kaen, Thailand
[*]Corresponding author: snath@kku.ac.th

Received 10 April 2021
Revised 15 October 2021
Accepted 31 October 2021

**Abstract**

Nuclear magnetic resonance (NMR) relaxation properties of four separate mangosteen tissues—normal flesh, translucent flesh, pericarp, and seed—were investigated to assess the potential application of NMR relaxometry in detecting translucent flesh disorder. Longitudinal and transverse relaxation signals from each tissue type of the tested mangosteens were collected using the inversion recovery (IR) and Carr–Purcell–Meiboom–Gill (CPMG) pulse sequences, respectively. Longitudinal relaxation time constant ($T_1$) spectra and transverse relaxation time constant ($T_2$) spectra of the four tissues were obtained using the free inverse Laplace transform software CONTIN. Analysis of the $T_1$ vs. $T_2$ distribution of the major peaks of the spectra revealed that the clusters of the normal flesh and translucent flesh were isolated, whereas the clusters of seed and pericarp tissue mostly overlapped. Clusters of normal and translucent flesh were distinguished via $T_2$ relaxation time at approximately 0.66 s at 21 MHz. Moreover, the NMR signal intensities of seed and pericarp were significantly lower than those of normal and translucent flesh. This technique may be usefully applied in detection of translucent flesh. However, detection of translucent flesh via $T_2$ relaxation time should be further verified in intact mangosteens before the approach sees practical application.

**Keywords:** Mangosteen, Translucent flesh disorder, NMR relaxometry, Time domain NMR, Inverse Laplace transform, CONTIN

## 1. Introduction

The mangosteen (*Garcinia mangostana* L.), a tropical fruit originating in Southeast Asia, is one of Thailand's major commercial fruit crops. The most critical quality-control challenge in mangosteen agriculture is the difficulty of detecting translucent flesh disorder, which produces crisp, abnormal tissue within affected fruit. The currently practiced method of detection relies upon visual judgments made after cutting and opening the peel of the mangosteen. Research groups have proposed three classes of alternative, non-destructive methods of detecting translucent flesh: 1) methods based on physical properties, 2) spectroscopy methods, and 3) imaging methods. Specific methods in the first class include a (water-) floating test, which relies on differences in specific gravity[1], as well a test based on electrical impedance [2] and one based on acoustic vibrational resonance [3]. However, these techniques are not reliable either as their accuracy varies according to skin color, size, and pericarp characteristics of the mangosteen assessed [3]. The second class, spectroscopy methods, includes microwave spectroscopy [4] as well as infrared and near-infrared (NIR) spectroscopy [5]. Imaging techniques such as X-ray computed tomography (CT) and magnetic resonance imaging (MRI) techniques are included in the third class [6].

In principle, imaging methods are the most accurate means of detecting translucent flesh because such flesh can be identified in both CT and MRI images. Nevertheless, instrument costs, operational complications, and very low throughput rates render these methods unsuitable in practice. Spectroscopy methods strike a balance between the high accuracy of the imaging methods and the low cost (and high throughput rate) of the physical properties-based methods; currently, the most prominent spectroscopy method involves analyzing infrared or

NIR transmittance spectra. The method has been reported as providing an rate of detection, though many factors can still confound detection accuracy [5]. NIR light passes through every part of the mangosteen, affecting the overall spectrum measured, and therefore, mangosteen characteristics such as size, peel hardness and thickness, gummy latex, and skin color can affect the results. The position and orientation of both the tested mangosteen and the infrared light source can also influence spectrum measurements [7].

Another technique capable of detecting translucent flesh in mangosteens is nuclear magnetic resonance (NMR). NMR relaxation techniques have been used for decades in time-domain nuclear magnetic resonance (TD-NMR) for the quality control of agricultural products [8] and petrochemical processes [9]. In mangosteens, the high water content of various cell-structure environments throughout the fruit provide the sources of NMR signal readings. In food or fruit, the water is not bulk water (characterized by a mono-exponential decay of $T_1$ and $T_2$ ) but rather compartmentalized water that gives rise to multiexponential decays which must be characterized by multiple time constants [10,11]. In TD-NMR, each relaxation component of the measured relaxation signal can be extracted by way of the numerical inverse Laplace transform [12]. However, to assess the possibility of using TD-NMR to detect translucent flesh, it is first necessary to understand the NMR relaxation properties of each part of the mangosteen. This research investigates such properties in each part of the mangosteen, including the translucent flesh, to evaluate the potential of TD-NMR relaxometry in detecting translucent flesh in mangosteens.

Water and oil are the primary sources of NMR signals in agricultural products, and water plays a particularly important role in the case of the mangosteen. Water in plant cell structure can be roughly classified into two types: bound water (BW), the water located in the cell wall and in intracellular spaces, and free water (FW), the water located in intercellular spaces [13]. BW has a short $T_2$ relaxation time; the $T_2$ relaxation time of FW is longer [14]. Since both exist in the plant cell, both affect the NMR relaxation times, and tissue that possesses a longer NMR relaxation time should be characterized by a larger quantity of FW. Translucent flesh in mangosteens has weak and insubstantial cell walls, and its intercellular space is larger than that of normal flesh [15]. Accordingly, NMR relaxation times are expected to vary between normal flesh and translucent flesh. Though water content can also vary according to the number of days since harvest, the NMR relaxation times $T_1$ and $T_2$ of the water molecules are, in this research, the primary point of distinction between mangosteen tissue types because the relaxation times correspond to the cell structure.

## 2. Materials and methods

### *2.1 Preparation of samples*

The 60 normal mangosteens and 20 translucent-flesh mangosteens used in this study were purchased from a local market in Khon Kaen, Thailand. From the normal mangosteens, 20 samples were taken of normal flesh, of seed tissue, and of pericarp tissue (60 samples from normal mangosteens), and from the translucent-flesh mangosteens, 20 samples of translucent flesh were taken, bringing the total number of samples to 80. All samples were cut and inserted into test tubes 5.0 mm in diameter to a height of approximately 10.0 mm. The NMR relaxation signal of each sample was collected via the PS2-B system (TeachSpin, New York, USA) at room temperature. The inversion recovery (IR) and Carr–Purcell–Meiboom–Gill (CPMG) pulse sequences were used to obtain $T_1$ and $T_2$ relaxation signals for each sample. The acquisition parameters of the IR pulse sequence were as follows: repetition time (TR) was 18 s, the shortest stepping time ($\tau$) of 0.05 ms was used, the number of data points was 120, and the number of signals averaged was 16. For the CPMG pulse sequence, acquisition parameters were as follows: echoes time (TE) was 1.2 ms, the number of echoes was 5000, TR was 20 s, and the number of signals averaged was 16.

### *2.2 NMR multi-exponential relaxation*

As mentioned previously, an acquired NMR relaxation signal is the sum of the relaxation of the many components of the tissue sample; this is known as multi-exponential relaxation. For biomaterials, the number of components of multi-exponential relaxation may be infinite, and thus, the measured $T_1$ relaxation signal $M_1(t)$ and $T_2$ relaxation signal $M_2(t)$ can be modeled as Laplace integrations [12]. These can be presented in a logarithmic scale, as in Equation 1 and Equation 2 [16],

$$M_1(t) = \int_0^\infty H(T_1)\left(1 - 2e^{-\frac{t}{T_1}}\right) d\,ln\,T_1 + C_1 \quad (1)$$

$$M_2(t) = \int_0^\infty K(T_2)e^{-\frac{t}{T_2}} d\,ln\,T_2 + C_2 \quad (2)$$

where $H(T_1)$ is a $T_1$ relaxation time distribution function and $K(T_2)$ is a $T_2$ relaxation time distribution function, while $C_1$ and $C_2$ are the background signals. Both $T_1$ and $T_2$ spectra can be obtained by inverting the Laplace integrations Equation 1 and Equation 2. For a noise-contributed signal, the CONTIN algorithm is reliable and widely used for inverse Laplace transforms [17]. In this research, the original CONTIN program was used to obtain the $T_1$ and $T_2$ distributions. To make the $T_1$ relaxation signals viable in the CONTIN program, the measured rising signals, $M_1(t)$, were first transformed into their decayed form, $M'_1(t)$, by using Equation 3,

$$M'_1(t) = \frac{M_1(t) - M_0}{2} = M_0 e^{-\frac{t}{T_1}} \quad (3)$$

where $M_0$ is the highest value of the signal.

*Slice preparation and cell structure imaging*

One sample of each tissue type was selected and prepared for cell structure imaging. Each was sectioned using a razor blade to obtain a thickness of approximately 0.5–1.0 mm to allow light to pass through, after which it was placed on a microscope slide with drops of distilled water and covered with a cover slip. The cell structure image was then taken with a camera attached to an optical microscope (namely a Canon EOS 800D on a Primo Star optical microscope).

## 3. Results and discussion

The transformed $T_1$ relaxation signals $M'_1(t)$ of the four tissue types and their corresponding $T_1$ distributions are shown in Figures 1 and 2, respectively, while the $T_2$ relaxation signals of the four tissue types and their corresponding $T_2$ spectra are shown in Figures 3 and 4, respectively. As Figures 1 to 4 show, the signal magnitudes of seed and pericarp were smaller, and decayed faster, than those of normal and translucent flesh. This is useful for the practical detection of translucent flesh in mangosteens: the signals of seed and pericarp do not dominate those generated by flesh tissue, and they can be easily excised.

The seeds and pericarp of mangosteens chiefly comprise carbohydrate and protein fiber in semi-solid states. These constituents have extremely short relaxation times, and neither IR nor CPMG approaches can detected them. Thus, the NMR signals of seed and pericarp—depicted in Figure 1 and Figure 3—are in fact largely the signals of water contained within the cell structures of the pericarp and seeds. Although the samples' masses were not controlled, their volumes were, which is sufficient to allow the comparison of the trend of proton density for each tissue. As NMR proton density is proportional to the magnitude of the early signal of the (IR or CPMG) sequence, averages of the first three points of each signal in Figure 1 were used to represent proton densities. The average intensity of early NMR signals was 0.8 for normal flesh, 0.9 for translucent flesh, 0.4 for seed tissue, and 0.4 for pericarp tissue (arbitrary units). Naturally, the proton densities of normal flesh and translucent flesh exceeded those of pericarp and seed; however, these cannot be used to distinguish the normal flesh from the translucent because there the difference between them was insignificant. The central location of the major peak of each spectrum was measured for each tissue. The results were used to plot the $T_1$ vs. $T_2$ distribution of the four tissue types, as presented in Figure 5. Only the major peak of each spectrum was considered in this work because in practical application with intact mangosteens, only the major peak of each tissue is expected to be detected in the measured relaxation spectra. The $T_1$ vs. $T_2$ distribution plot revealed that the cluster centers ($T_2$, $T_1$) of the translucent flesh, normal flesh, pericarp, and seed were (0.918, 1.199), (0.575, 0.998), (0.132, 0.194), and (0.278, 0.140) s, respectively. The range of variation in the pericarp cluster was substantial, which is to be expected in light of the pericarp's has highly heterogeneous tissue structure in comparison with the others (Figure 6). The seed and pericarp clusters mostly overlapped, while the clusters of normal flesh and translucent flesh were isolated.

The fact that the $T_2$ relaxation time of the translucent flesh was longer than that of the normal flesh implies that the former tissue contains a larger amount of free water than the latter. Figure 6B illustrates that the translucent flesh has a weak and insubstantial cell wall. Unfortunately, the intercellular space of the tissue was obscured in the photograph; nevertheless, evidence illustrating that the intercellular space of the translucent flesh is larger than that of normal flesh can be found in the transmission electron microscopy images of the Paopun report [15]. Moreover, according to the Brownstein and Tarr model [18], the translucent flesh's larger cell size (Figure 6 (B)) is another contributing factor to the longer $T_1$ and $T_2$ relaxation times of translucent flesh. According to the $T_1$ vs. $T_2$ distribution plot in Figure 5, the normal flesh and the translucent flesh clusters can be distinguished by $T_2$ relaxation times at approximately 0.66 s at 21 MHz. This suggests that TD-NMR is a viable means of detecting translucent flesh disorder in mangosteens. The use of $T_2$ relaxation time to detect the translucent flesh offers two advantages. First, the $T_2$ relaxation signal acquired via the CPMG sequence contains many data points, which are helpful in obtaining a confident result from the CONTIN inverse Laplace

transform. Second, the CPMG signal acquisition time is short, which will improve the throughput rate of the detection process. Having confirmed the potential utility of TD-NMR in detecting translucent flesh, this research opens the door to the next step towards practical application: investigating the method's detection rate in intact mangosteens. Although low-field NMR instruments can currently be made in-house at a low cost, some automatic processes—such as frequency tuning and pulse calibration—must also be developed for automatic detection to be successful.

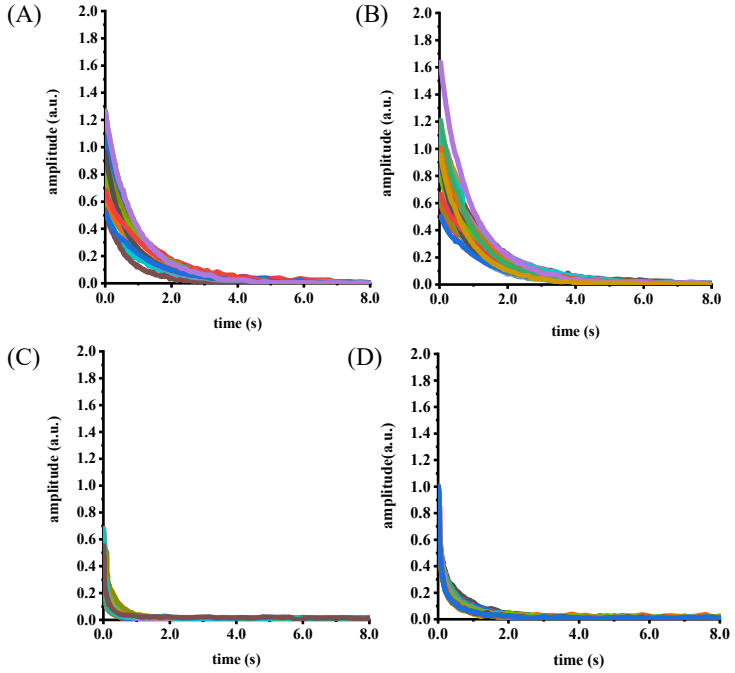


**Figure 1** The transformed $T_1$ relaxation signals of (A) normal flesh, (B) translucent flesh, (C) seeds, and (D) pericarps of the tested mangosteens, 20 curves per tissue.

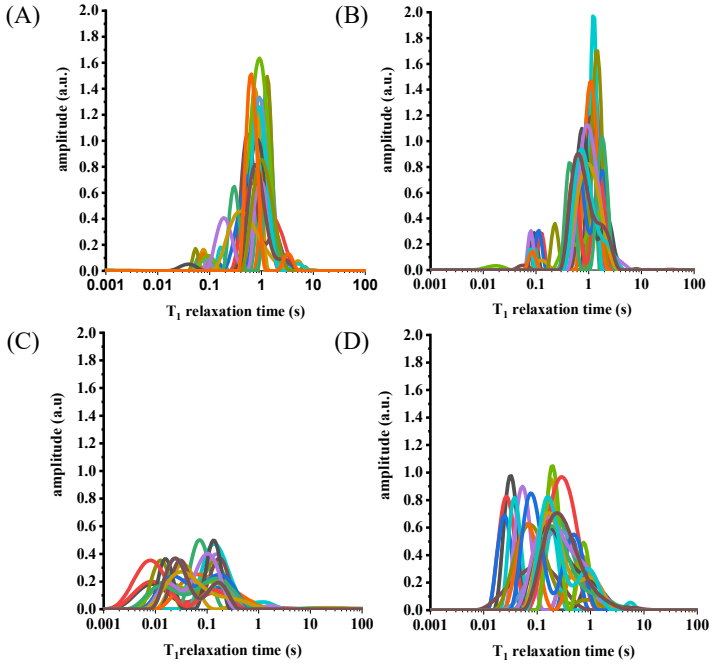


**Figure 2** The corresponding $T_1$ spectra of (A) normal flesh, (B) translucent flesh, (C) seeds, and (D) pericarps of the tested mangosteens, 20 curves per tissue.

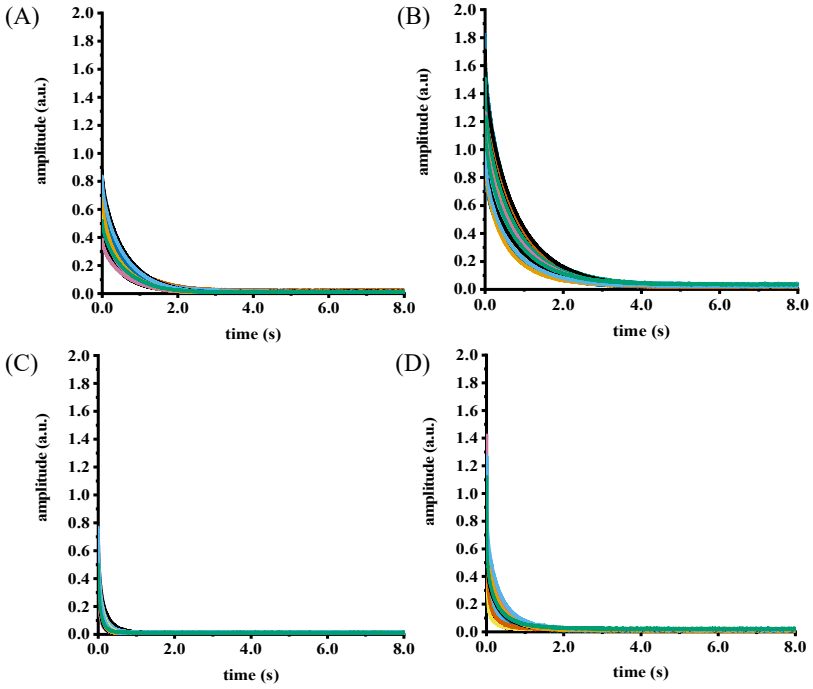


**Figure 3** $T_2$ relaxation signals of (A) normal flesh, (B) translucent flesh, (C) seed, and (D) pericarp of the tested mangosteens.

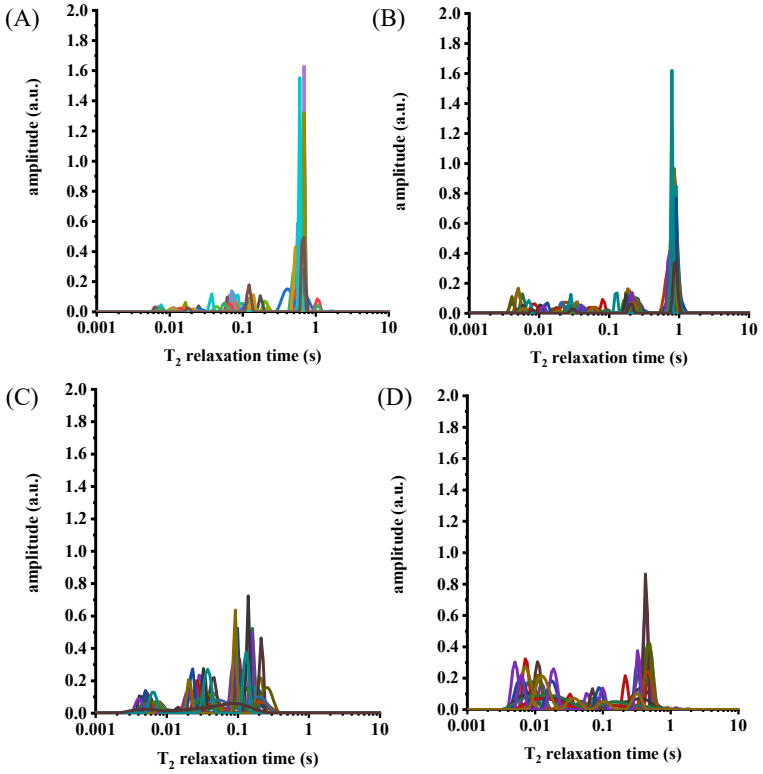


**Figure 4** The corresponding $T_2$ spectra of (A) normal flesh, (B) translucent flesh, (C) seed, and (D) pericarp of the tested mangosteens.

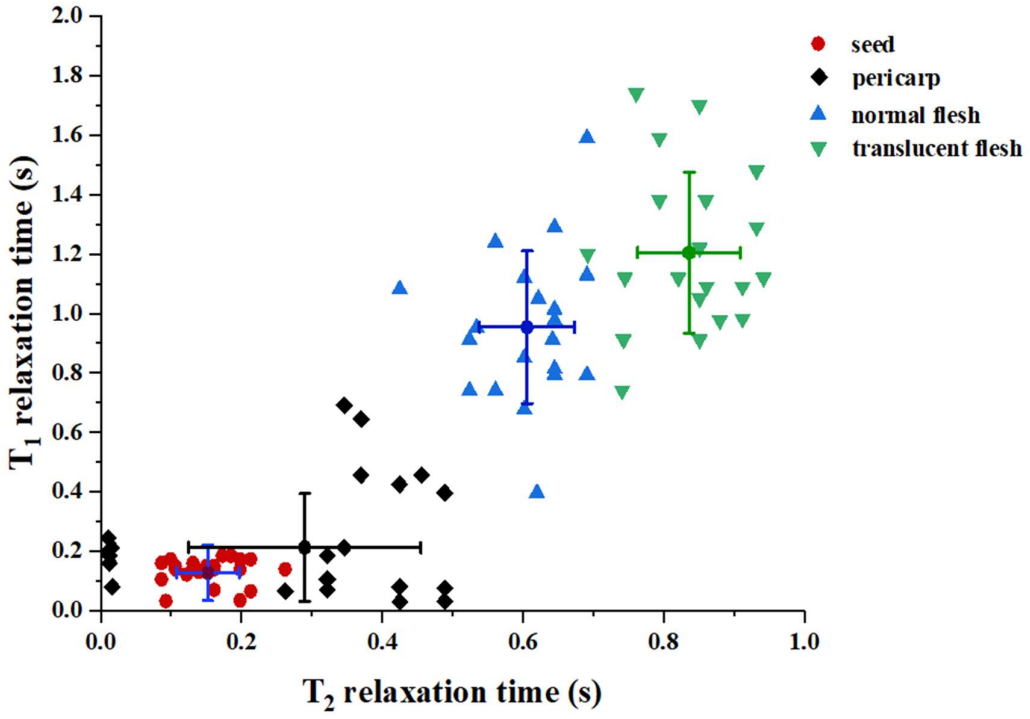


**Figure 5** Scatter plot of the major peak positions of the $T_1$ and $T_2$ spectra of the four tissue types. Horizontal and vertical error bars represent $T_2$ and $T_1$ standard deviations, respectively, of each tissue.

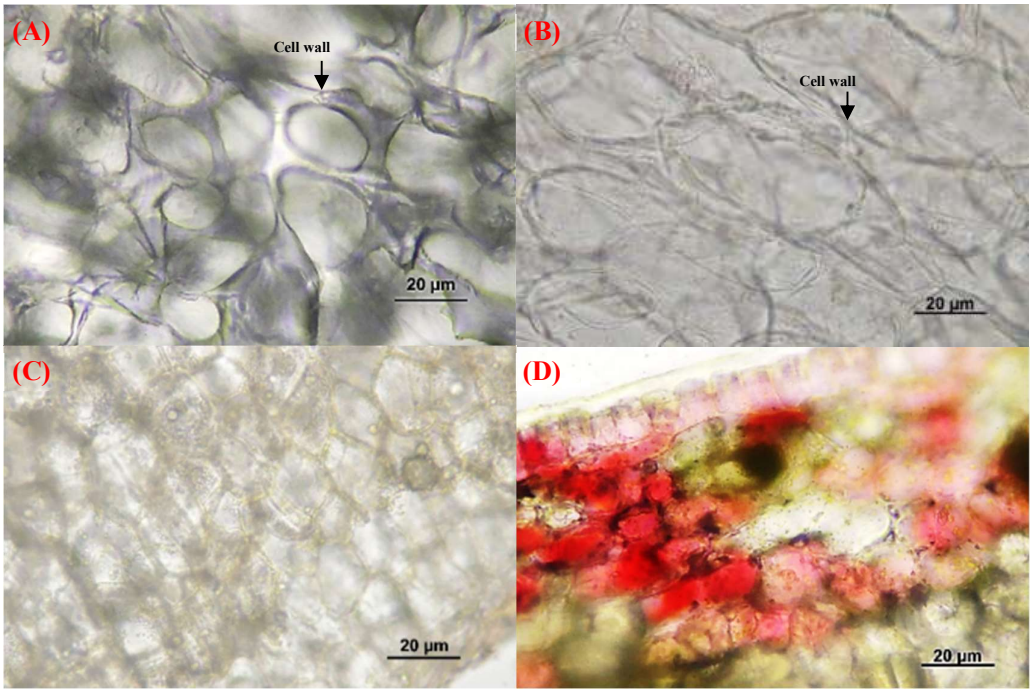


**Figure 6** Microstructure picture of mangosteen tissue—(A) normal flesh, (B) translucent flesh, (C) seed, and (D) pericarp—obtained with an optical microscope (Primo Star optical microscope; Canon EOS 800D camera).

## 4. Conclusion

Four mangosteen tissue types—normal flesh, translucent flesh, pericarp, and seed—were investigated by separately measuring the NMR signals of each. Seed and pericarp had relatively low signal intensities and short relaxation times, which can reasonably be ignored in translucent flesh detection. Pericarp, owing to its

heterogeneous tissue structure, produced a wide variety of relaxation times. Translucent flesh yielded the highest proton density and NMR signal intensity, possibly because of excess water. It also had the highest $T_1$ and $T_2$ relaxation times, corresponding to its larger cell size and portion of free water. In NMR experiments at 21 MHz, the translucent flesh was successfully distinguished from the other tissues by means of $T_2$ relaxation time at a threshold of approximately 0.66 s.

## 5. Acknowledgments

The authors would like to thank the Department of Physics, Faculty of Science, Khon Kaen University for providing all of the research facilities; and Ms. Sudathip Saensupha for assisting with the cell structure imaging capture and microscope slide preparation.

## 6. Referrences

[1] Pankasemsuk T, Garner JO, Matta FB, Silva JL. Translucent flesh disorder of mangosteen fruit (*Garcinia mangostana* L.). Hort Sci. 1996;31(1):112-113.

[2] Nakawajana N, Terdwongworakul A, Teerachaichayut S. Minimally destructive assessment of mangosteen translucency based on electrical impedance measurements. J Food Eng. 2016;171:137-144.

[3] Jaritngam R, Limsakul C, Wongkittiserksa B. The relation between the texture properties of mangosteen (*Garcinia mangostana* Linn.) And the resonance frequency in detection of the translucent and yellow gummy latex. Emirates J Food Agric. 2013;25:89-96.

[4] Tongleam T, Jittiwarangkul N, Kumhom P, Chamnongthai K. Non-destructive grading of mangosteen by using microwave moisture sensing. In: Itoh Y, Dejhan K, editors. International Symposium on Communications and Information Technology (ISCIT); 2004 Oct 26-29; Sapporo, Japan. New York: IEEE; 2004. p. 650-653.

[5] Teerachaichayut S, Kil KY, Terdwongworakul A, Thanapase W, Nakanishi Y. Non-destructive prediction of translucent flesh disorder in intact mangosteen by short wavelength near infrared spectroscopy. Postharvest Biol Tech. 2007;43(2):202-206.

[6] Yantarasri T, Sornsrivichai J, Chen P. X-ray and NMR for nondestructive internal quality evaluation of durian and mangosteen fruits. In: Bieleski R, Liang W, Clark, editors. International Postharvest Science Conference Postharvest 96; 1998 Mar 1; Taupo, New Zeland. Leuven: ISHS; 1998. p. 97-102.

[7] Terdwongworakul A, Nakawajana N, Teerachaichayut S, Janhiran A. Determination of translucent content in mangosteen by means of near infrared transmittance. J Food Eng. 2012;109(1):114-119.

[8] Colnago LA, Wiesman Z, Pages G, Musse M, Monaretto T, Windt CW, et al. Low field, time domain NMR in the agriculture and agrifood sectors: an overview of applications in plants, foods and biofuels. J Magn Reson. 2021;323:106899.

[9] Rudszuck T, Förster E, Nirschl H, Guthausen G. Low-field NMR for quality control on oils. Magn Reson Chem. 2019;57(10):777-793.

[10] Snaar JEM, Van As H. Probing water compartments and membrane permeability in plant cells by 1H NMR relaxation measurements. Biophys J. 1992;63(6):1654-1658.

[11] Hills BP. Applications of low-field NMR to food science. In: Webb GA, editor. Annual reports on NMR spectroscopy. 58th ed. Massachusetts: Academic Press; 2006. p. 177-230.

[12] Berman P, Levi O, Parmet Y, Saunders M, Wiesman Z. Laplace Inversion of low-resolution NMR relaxometry data using sparse representation methods. Concepts Magn Reson Part A Bridg Educ Res. 2013;42(3):72-88.

[13] Joardder MUH, Kumar C, Karim MA. Food structure: its formation and relationships with other properties. Crit Rev Food Sci Nutr. 2017;57(6):1190-1205.

[14] Khan MIH, Wellard RM, Nagy SA, Joardder MUH, Karim MA. Investigation of bound and free water in plant-based food material using NMR $T_2$ relaxometry. Innov Food Sci Emerg Technol. 2016;38:252-261.

[15] Paopun Y, Umrung P, Thanomchat P. Cell wall structure of translucent cells of mangosteen fruit. In: Poovarodom S, Yingjajaval S, ediors.VII International Symposium on Mineral Nutrition of Fruit Crops; 2013 May 19; Chanthaburi, Thailand. Leuven: ISHS; 2013. p. 421-426.

[16] Mao R, Tang J, Swanson BG. Relaxation time spectrum of hydrogels by CONTIN analysis. J Food Sci. 2000;65:374-381.

[17] Provencher SW. CONTIN: a general purpose constrained regularization program for inverting noisy linear algebraic and integral equations. Comput Phys Commun. 1982;27(3):229-242.

[18] Brownstein KR, Tarr CE. Importance of classical diffusion in NMR studies of water in biological cells. Phys Rev A.1979;19(6):2446-2453.